Legged Elastic Multibody Systems: Adjusting Limit Cycles to Close-to-Optimal Energy Efficiency

Philipp Stratmann[1,2], Dominic Lakatos[2], Mehmet C. Özparpucu[2], Alin Albu-Schäffer[1,2]

***Abstract*—Compliant elements in robotic systems can strongly increase the energy efficiency of highly dynamic periodic motions with large energy consumption such as jumping. Their control is a challenging task for multi-joint systems. Typical control algorithms are model-based and thus fail to adjust to unexpected mechanical environments or make limited use of mechanical resonance properties. Here, we apply numerical optimal control theory to demonstrate that close-to-optimal energy-efficient movements can be induced from a one-dimensional sub-manifold in jumping systems that show nonlinear hybrid dynamics. Linear weights transform sensory information into this one-dimensional controller space and reverse transform one-dimensional motor signals back into the multi-dimensional joint space. In Monte-Carlo-based simulations and experiments, we show that an algorithm that we derived previously can extract these weights online from sensory information about joint positions of a moving system. The algorithm is computationally cheap, modular, and adjusts to varying mechanical conditions. Our results demonstrate that it reduces the problem of energy-efficient control of multiple compliant joints that move with high synchronicity to a low-dimensional task.**

***Index Terms*—Compliance and impedance control, redundant robots, Optimization and Optimal Control.**

I. INTRODUCTION

ROBOTIC platforms are increasingly equipped with compliance in their actuators, which allow to store energy and release it at a later time to increase the energy efficiency of a given movement. These elastic properties significantly influence the dynamics of an actuator at high velocity and force during highly dynamic cyclic movements such as jumping. Different strategies have been proposed to control robots that comprise compliant actuators and multiple degrees of freedom. Most approaches rely on a model and a fixed set of considered initial conditions [1], such as algorithms based on *Poincaré-maps* [2], transverse linearization [3] or optimal control [4]. They lack the ability to adjust to unexpected conditions and environments. Algorithms based on *van der Pol* oscillators often use a nonlinear damping term to enforce a pre-defined limit cycle [5], [6]. This term artificially introduces energy losses and changes the dynamics of the system, which reduces the movement efficiency. An approach to overcome these problems are central pattern generators (CPGs) that mimic animal locomotion control by outputting a default motor signal which adapts according to sensory input. Typically, all joints are driven by individual CPGs that are coupled among each other [7], [8], [9]. These studies focus on the phase relation of the CPGs, but neglect tuning of the relative motor strength, which has a strong influence on the energy efficiency [10].

We have recently demonstrated that under specific intrinsic damping properties of the actuators, the stable control of robotic platforms with several joints may be reduced to a one-dimensional control problem during highly dynamic movements [11], [12]. The algorithm linearly transforms sensory input from the multi-dimensional joint space into a one-dimensional controller space. We analytically derived a learning rule to extract transformation weights which are the optimal, local, linear approximation of the mode of the system in a least-squared sense [11]. The obtained formula is mathematically equivalent to the well-analyzed *Oja's rule* [13], [14]. The input entrains a bang-bang unit, and its motor output is reversely transformed into the joint space. The binary nature of the bang-bang control guarantees convergence to a stable limit cycle within few oscillation periods, as extensively validated both analytically [15] and experimentally [11], [16]. Our approach extends the previous literature by an algorithm that requires neither a priori knowledge of model parameters nor artificial damping. The performed calculations are computationally simple and require to store only the modal transformation weights during execution. The sensory requirements are limited to information about joint forces and positions. Additionally, the chosen modal coordinate transformation is analytically known to allow for resonant relative motor strengths in certain ideal mechanical systems, where it thus achieves a highly energy efficient actuation [11]. We will hereby denote a control law as *energy-efficient* if it maximizes the amplitude of a movement for an energy input of pre-defined magnitude. In particular, the modal weights allow resonant movement in undamped linear mechanical systems which are formed of n elastically coupled bodies, that can be described by a constant diagonal inertia matrix, and which are subject to modal damping and white noise. Such a system has n eigenfrequencies and associated normal modes. If we repeatedly excite the system by deviating all springs simultaneously along any of the eigenmodes, all masses will oscillate in phase with the corresponding eigenfrequency, i.e. mechanical resonance occurs. Oja's rule derives the dominant principal

Manuscript received: September, 09, 2016; Accepted November, 12, 2016.
This paper was recommended for publication by Editor Paolo Rocco upon evaluation of the Associate Editor and Reviewers' comments.

[1]Department of Informatics, Technical University of Munich, 85748 Garching, Germany.
[2]Institute of Robotics and Mechatronics, German Aerospace Center (DLR), Muenchener Strasse 20, 82234 Wessling, Germany.
Contact: philipp.stratmann@dlr.de

Digital Object Identifier (DOI): see top of this page.

component, corresponding to the physical eigenmode that shows the maximum amplitude for the described mechanical system [17], [18]. For a random initial excitation, this is most likely the least damped eigenmode. The performance of Oja's rule is improved by the fact that the bang-bang control inserts energy along the iteratively extracted modal weights, thereby forming a positive feedback loop that enhances the amplitude of the particular mode. In the controller space formed by transformation weights that are extracted by Oja's rule, a one-dimensional timing signal can thus excite all bodies along the least-damped resonant mode. We expect that the modal transformation also allows the control of energy-efficient movement in systems with more general nonlinear dynamics. This is due to the fact that the dominant principle component is the least-square-optimal linear approximation to a data set describing the dynamics [19], which implies that the modal excitation enables close-to-optimal control during the short phase of energy insertion by the bang-bang law.

The present study focuses on the energy optimality of the proposed modal transformation for hybrid compliant mechanical systems subject to nonlinear dynamics. The considerations are based on a periodically jumping leg with two joints, since locomotion bears particular potential for optimization by compliant structures due to its high energy consumption and high occurring impact forces. The hypothesis that our controller induces energy-optimal movement can be divided into three aspects that will be tested individually: Firstly, optimized jumping height is obtained in a stable limit cycle for a modal control approach. A control law that optimizes particularly the last jump in a sequence leads to a periodic trajectory in the preceding jumps and implicitly optimizes each preceding jump individually. Secondly, the optimal transformation weights are constant in time under fixed mechanical conditions. Thirdly, Oja's rule can extract the optimal weights during modally driven jumping movement. We validate the first two assumptions by numerically deriving an optimal control using a Legendre-Gauss-Radau quadrature orthogonal collocation method as implemented in *GPOPS-II* [20]. In a second step, we use a Monte Carlo method to verify that Oja's rule extracts the energy-optimal transformation weights online from sensory signals. We concentrate on a bang-bang control in the controller space as this is the key to the previously observed high movement stability.

In combination with our previous work, we conclude that Oja's rule allows to reduce the generation of stable, adaptable, and energy-efficient movement in multiple compliant joints to a low-dimensional problem. The algorithm may be used in the control of robotic platforms with multiple actuated links as a simple module that adjusts the intra-limb coordination to mechanical changes. Hereby, it optimizes the energy efficiency both of the mechanical actuators and the hardware required to calculate the control law.

II. THE CONTROL ALGORITHM

The modally adaptive bang-bang controller that we recently described [11], [12] controls a multi-body system with n joints driven by series elastic actuators (SEAs). A movement is initiated by deflecting the system from its equilibrium position. The controller observes the movement and adjusts it iteratively until it converges to a stable limit cycle. For this purpose, the controller receives information about the joint torques $\boldsymbol{\tau} \in \mathbb{R}^n$, which are a function of the difference between link and motor coordinates $\boldsymbol{q}, \boldsymbol{\theta} \in \mathbb{R}^n$, respectively,

$$\boldsymbol{\tau} = \boldsymbol{\tau}(\boldsymbol{\theta} - \boldsymbol{q}) \ . \tag{1}$$

The torque is transformed from the joint space into a one-dimensional sub-manifold along the modal weights $\boldsymbol{w} \in \mathbb{R}^n$,

$$\tau_{\mathrm{z}} = \frac{\boldsymbol{w}^T}{\|\boldsymbol{w}\|}\boldsymbol{\tau} \ . \tag{2}$$

Here, it triggers the controller of constant amplitude and threshold $\hat{\theta}_{\mathrm{z}}, \epsilon_\tau \in \mathbb{R}$, respectively,

$$\theta_{\mathrm{z}} = \begin{cases} +\hat{\theta}_{\mathrm{z}} & \text{if } \tau_{\mathrm{z}} > \epsilon_\tau \\ 0 & \text{if } -\epsilon_\tau \leq \tau_{\mathrm{z}} \leq \epsilon_\tau \\ -\hat{\theta}_{\mathrm{z}} & \text{if } \tau_{\mathrm{z}} < -\epsilon_\tau \end{cases} \ . \tag{3}$$

The output is transformed back into the joint space and the motor positions are accordingly updated to

$$\boldsymbol{\theta} = \frac{\boldsymbol{w}}{\|\boldsymbol{w}\|}\theta_{\mathrm{z}} \ . \tag{4}$$

The linear transformation weights are recursively extracted from the joint trajectories according to the learning rule,

$$\dot{\boldsymbol{w}}(t) = \gamma(\boldsymbol{w}(t)^T\boldsymbol{q}(t))\left[\boldsymbol{q}(t) - (\boldsymbol{w}(t)^T\boldsymbol{q}(t))\boldsymbol{w}(t)\right] \ , \tag{5}$$

which is mathematically equivalent to Oja's rule [13]. The adjustment rate γ is chosen smaller than the period frequency of the movement to capture the dynamics of the system during the whole movement cycle.

This study extends the previous description and analysis of the presented control law by energetic considerations. We restrict our simulations to mechanical systems where each actuator comprises a torsional spring with same constant stiffness $k \in \mathbb{R}$. Crossing the threshold $\pm\epsilon_\tau$ switches the torque,

$$\boldsymbol{\tau}_0 = k(-\boldsymbol{q}) \ \rightarrow \ \boldsymbol{\tau}_1 = k\left(\frac{\boldsymbol{w}}{\|\boldsymbol{w}\|}\left[\pm\theta_{\mathrm{z}}\right] - \boldsymbol{q}\right) \ .$$

The performed work equals the change of potential energy,

$$c_{\epsilon\hat{\theta}} = \frac{1}{2}\frac{\boldsymbol{\tau}_1^2}{k} - \frac{1}{2}\frac{\boldsymbol{\tau}_0^2}{k} \tag{6}$$

$$= \mp k\hat{\theta}_{\mathrm{z}}\frac{\boldsymbol{w}^T}{\|\boldsymbol{w}\|}\boldsymbol{q} + \frac{1}{2}k\hat{\theta}_{\mathrm{z}}^2 = \epsilon_\tau\hat{\theta}_{\mathrm{z}} + \frac{1}{2}k\hat{\theta}_{\mathrm{z}}^2 \ . \tag{7}$$

Equation (7) illustrates that the controller amplitude $\hat{\theta}_{\mathrm{z}}$ and threshold ϵ_τ define the energy inserted into the mechanical system. They determine whether the actuated system converges to a limit cycle or falls silent. The latter happens when the modal torque fails to reach the switching threshold.

III. OPTIMALITY OF THE LIMIT CYCLE

In the following sections, we test three aspects of energy efficiency: Here, we check whether optimization of individual jumps is achieved during a limit cycle. Subsequently, whether the energy-optimal modal transformation weights are time-invariant. Finally, whether a bang-bang controller in combination with Oja's rule extracts the optimal transformation weights from sensory information.

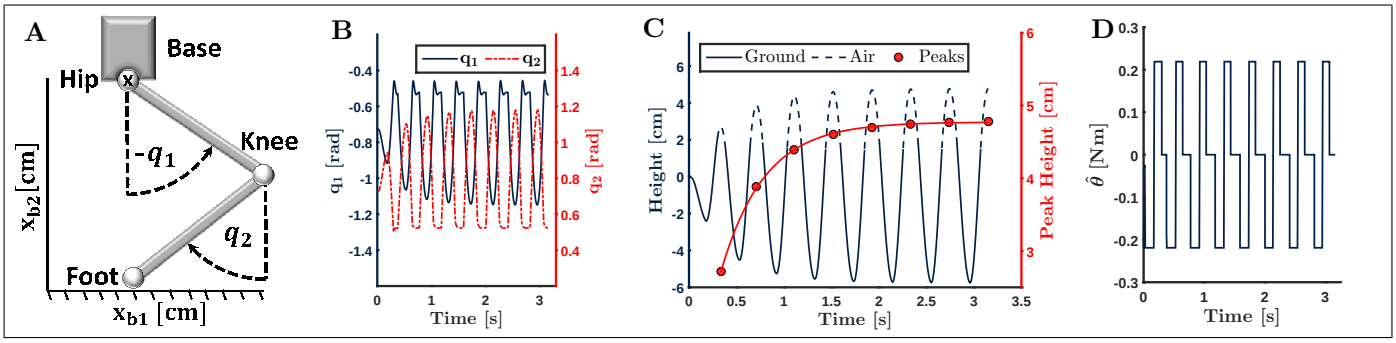

Fig. 1. **(A)** The mechanical test bed consists of a base that is serially connected to two links by a hip and a knee joint. The base coordinates $(x_{\mathrm{b1}}, x_{\mathrm{b2}})$ are measured at the middle of the hip joint, as indicated by an $\boldsymbol{x}$ in the illustration. Joint coordinates (q_1, q_2) are measured clockwise relative to vertically extended links. **(B)** Illustration of movement induced by the optimal controller obtained under the constraint of time-independent transformation weights represented by the weight angle α. Plotted here are the joint coordinates. **(C)** A plot of the resulting trunk trajectory indicates that after eight jumps the trajectory of the leg has approximately converged to a limit cycle. We extracted the peak heights of the jumping movement and plotted them together with a line showing an exponential fit against the second, right y-axis with higher resolution. **(D)** The derived controller is plotted for the whole simulated time. While it is artificially fixed to zero during flying phases, we find clear bang-bang behavior during the standing phase.

A. Methods

Mechanical System: As example system for our considerations, we simulate a floating base with one leg (cf. Fig. 1A) that models the robotic system used for the experimental validation in Sect. V. The floating base can freely translate in a vertical plane and we describe its position by $\boldsymbol{x}_{\mathrm{b}} = (x_{\mathrm{b1}}, x_{\mathrm{b2}})^T \in \mathbb{R}^2$. A trunk of mass $0.49\mathrm{kg}$ is attached by a hip joint to a leg. The leg comprises an upper and lower thigh that have respective masses of $0.059\mathrm{kg}$ and $0.038\mathrm{kg}$, equal length of $8\mathrm{cm}$, and are connected serially by one knee joint. Parameters describing the inertia are obtained from the CAD model of the robot. The respective joint coordinates q_1 and q_2 of the hip and knee joint are measured relative to a vertical orientation of the upper and lower link. We summarize joint and floating base coordinates as $\boldsymbol{x} = (\boldsymbol{x}_{\mathrm{b}}^T, \boldsymbol{q}^T)^T \in \mathbb{R}^4$. The joints are driven by series elastic actuators (SEAs) comprising torsional springs of constant stiffness $k = 1.46\mathrm{N\,m\,rad^{-1}}$ and damping coefficient $c = 0.0219\mathrm{N\,m\,s\,rad^{-1}}$. The actuators deviate the springs by an angle $\boldsymbol{\theta}$ from their equilibrium position. One SEA directly actuates the hip joint, while the second is connected to the knee via a belt drive. The resulting kinematic coupling allows for an independent influence of the SEAs on either joint coordinate [21]. Thus, we can describe the system by

$$\boldsymbol{M}(\boldsymbol{x})\ddot{\boldsymbol{x}} + \boldsymbol{C}(\boldsymbol{x}, \dot{\boldsymbol{x}})\dot{\boldsymbol{x}} + \boldsymbol{g}(\boldsymbol{x}) = \begin{pmatrix} \boldsymbol{0} \\ k(\boldsymbol{\theta} - \boldsymbol{q}) - c\dot{\boldsymbol{q}} \end{pmatrix} + \boldsymbol{\tau}_{\mathrm{contact}} \tag{8}$$

The symmetric, positive definite inertia matrix is denoted by $\boldsymbol{M}(\boldsymbol{x})$, $\boldsymbol{C}(\boldsymbol{x}, \dot{\boldsymbol{x}})$ represents the generalized Coriolis and centrifugal matrix, $\boldsymbol{g}(\boldsymbol{x})$ gravitational forces, and $\boldsymbol{\tau}_{\mathrm{contact}}$ the generalized external force. We describe the controller

$$\boldsymbol{\theta} = \hat{\theta}\frac{\boldsymbol{w}}{\|\boldsymbol{w}\|} = \hat{\theta}\begin{pmatrix} \sin(\alpha) \\ \cos(\alpha) \end{pmatrix} \tag{9}$$

by its Euclidean norm, $\hat{\theta} \in \mathbb{R}_{\geq 0}$, and the angle of the transformation weights, $\alpha \in [\pi, 2\pi]$. The constraint on α prevents ambiguity, since a change of α by π corresponds to a change of sign in $\hat{\theta}$. During jumping movement, the leg forms a hybrid model and alternatively switches between a standing and flying phase. During the contact phase, the foot and the ground form a fixed, unilateral contact point. We apply a rigid ground model because the differential equation solver restricts the use of stiff differential equations. Base rotation is locked, since in the long run we are interested in multi-legged systems. These systems have a high trunk inertia and can adjust their rotation independently from the jumping due to redundant degrees of freedom. Our choice results in fully actuated system dynamics during the stance phase, i.e. the number of actuators equals the number of degrees of freedom of the system. The initial position is defined by a vertical alignment of base and foot. While the foot is initially attached to the ground, we choose the height of the base that prevents any initial vertical acceleration on the trunk. Lift-off occurs when the vertical projection of the force constraining the foot to the ground switches its sign, whereas landing takes place upon ground contact.

Numerical Extraction of Optimal Controller: To find the optimal control law in the modal sub-manifold, we search for the optimal parameter α^* and piece-wise continuous control $\hat{\theta}^*(t)$. By *optimal* we hereby imply that for time-constant α the objective function is minimized, which is given in Mayer form by the negative jumping height

$$\mathcal{J}(\alpha, \hat{\theta}(t)) = -x_{\mathrm{b2}}(t_{\mathrm{end}}) \ . \tag{10}$$

For this purpose, we use a numerical approach for the optimal control of time-continuous multiple-phase dynamical systems as implemented in *GPOPS-II* [20]. The state of the mechanical system is described by $(\boldsymbol{x}^T, \dot{\boldsymbol{x}}^T)$ and the state equation $\boldsymbol{f} = \left(\dot{\boldsymbol{x}}^T, \ddot{\boldsymbol{x}}^T\right)^T$ is obtained from (8). According to the *hp-adaptive Gaussian quadrature collocation* method, GPOPS-II divides the time interval of interest into specific mesh points and discretizes the state at these points. The optimal control problem is then transformed into a nonlinear programming problem and is solved using IPOPT [22]. States are estimated using Lagrange polynomials, and both the number of mesh points and the degree of the polynomial are dynamically adjusted. We allow for a maximal simulated time of $6\mathrm{s}$ and 8 consecutive jumps, which we empirically found to be the maximum number supported by GPOPS-II. The control is only

active during the standing phase and the control set is given by $\alpha \in [\pi, 2\pi]$ as described before and $\hat{\theta} \in [-0.15\text{rad}, 0.15\text{rad}]$. The latter constraint restricts the spring deflections that the controller can induce equivalently to the bang-bang amplitude in (3). The energy inserted during a controller switching decreases linearly with $\boldsymbol{w}^T\boldsymbol{q}$. It is therefore maximized when the joint positions $\boldsymbol{q}$ and the weights $\boldsymbol{w}$ have opposite directions and $\boldsymbol{q}$ has maximum amplitude. A given spring deflection of amplitude $\hat{\theta}_z$ thus inserts the maximum energy at peak positions of $\boldsymbol{q}$, which means that for a given maximum value for $\hat{\theta}_\text{z}$ we induce the maximum energy when deflecting the springs instantaneously at the according point in time. The constraint accordingly renders it likely that the derived optimal controller amplitude $\hat{\theta}^*(t)$ will show bang-bang behavior.

B. Results

The derived optimal trajectory requires less than 6s to reach its peak jumping height, which indicates that time does not limit the performance of the derived controller.

As illustrated in Fig. 1B and 1C, the jumping trajectory approximately converges to a limit cycle with duration $T \approx 0.41\text{s}$. The difference between two successive peak heights of the trajectory decreases monotonically. An exponential fit, plotted in the same figure, indicates that the jumping height converges to a final value of 4.77cm. Convergence takes place with a time constant of approximately 2.19s. The optimal transformation weights are represented by $\alpha^* = 1.75\pi$, which corresponds to $(1, -1)^T$ as represented in the spanning set formed by the joint coordinates. This can be considered as a linear eigenvector of the nonlinear system. The orthogonal second eigenvector of the two-dimensional system would be described by $\alpha_{\text{EV2}} = 0.25\pi$. The controller $\hat{\theta}$ shows clear bang-bang-behavior and switches instantly from the minimum to maximum value of the controller set, as demonstrated in Fig. 1D. The switching occurs when the trunk crosses its lowest position with a time difference of $\Delta t < 9.4\text{ms} \approx 0\,02T$ (restricted by the numerical resolution). According to (7), the optimal controller thus inserts the same maximum possible energy into the system during each jump and not just during the final one. All of these findings indicate that the optimal controller, which maximizes the movement amplitude of the final jump, follows the same law during each of the preceding jumps. The goal of optimizing the height of an individual jump therefore requires to optimize each of the preceding jumps, which is achieved in a periodic movement. If only the final standing phase had an influence on the final jumping height, we would expect the controller to insert arbitrary amounts of energy during the earlier phases. All of these findings in summary indicate that a series of equivalently actuated preceding jumps induces maximum movement amplitude and an optimal controller leads to periodic movement.

The results furthermore emphasize the intrinsic stability of our control approach. For a given maximal amplitude $\hat{\theta}_\text{z}$, the obtained controller represents a version of our suggested algorithm where α and ϵ_τ are chosen to insert the maximum energy in the most energy-efficient way. Under this extreme condition, the trajectory still converges.

IV. OPTIMALITY OF THE MODAL TRANSFORMATION

We turn the focus to the linear weights of the mapping between the sensory/actuation and controller space. We will first investigate the influence that deviations from the optimal weights have on the controller performance and then test the second assumption of our approach, i.e. that the weights can be assumed constant during the movement cycle.

A. Methods

Deviations from Optimal Value: Using the same mechanical system as described in Sect. III-A, we fix α to 18 equally spaced values within $[1.1\text{rad}, 1.95\text{rad}]$ and leave the remaining parameters of the optimal control problem unchanged. For each trial, the final jumping height is recorded.

Influence of Time Independency: To check whether the optimal transformation weights are time-independent, we allow for $\alpha = \alpha(t)$ and use GPOPS-II to search for $\hat{\theta}^*(t)$ and $\alpha^*(t)$ that maximize the jumping height. All other conditions remain unchanged. Resonance in a linear two-dimensional system would require to drive the system along a constant eigenmode. In an additional trial, we test if a potentially observed deviation from the linearized expectation $\alpha^*(t) = \alpha_{\text{EV1}}$ results from coupling between the linearized eigenmodes either in the inertia matrix $\boldsymbol{M}(\boldsymbol{x})$ or the Coriolis and centrifugal matrix $\boldsymbol{C}(\boldsymbol{x}, \dot{\boldsymbol{x}})$. For this purpose, we reduce the masses of the links to zero. Since the numerically obtained eigenmode $(1, -1)^T$ induces a straight vertical jumping movement of the base in this system, a deviation would be due to coupling in the Coriolis and centrifugal force.

B. Results

Deviations from Optimal Value: When the transformation angle is fixed to different values, the optimal amplitude $\hat{\theta}^*(t)$ remains bang-bang (not illustrated). Figure 2A demonstrates that the maximum jumping height varies between 1.82cm and 4.78cm for different angles. For the current mechanical configuration, weight variations thus allow performance increases in terms of jumping height of up to 263%.

Influence of Time Independency: The optimal controller $\hat{\theta}^*(t)$ continues to show bang-bang-like behavior also under time-varying transformation weights, as illustrated in Fig. 2B. While $\alpha^*(t)$ remains equal to α_{EV1} directly after landing and before take-off for a major proportion of the trajectory, $\alpha^*(t)$ deviates from the linear eigenvector when the joints are increasingly deviated from their equilibrium position. At the point of maximum deviation, i.e. the minimum trunk height, both $\alpha^*(t)$ and $\hat{\theta}^*(t)$ are discontinuous. Expressed in Cartesian coordinates as represented by $\boldsymbol{\theta}(t)$ in (9), the controller describes a continuous semicircle during the standing phase before it is switched off at onset of the flying phase. The time-variation in transformation weights leads to an increase of the final jumping height of 1.9% in comparison to constant weights. The trajectory of the base, shown in Fig. 2C, is a loop. When the link masses are reduced to zero, this behavior remains (cf. same figure). For both systems, it is thus advantageous to insert some energy via the empirically derived eigenmode $(1, 1)^T$ at larger joint deflections, although

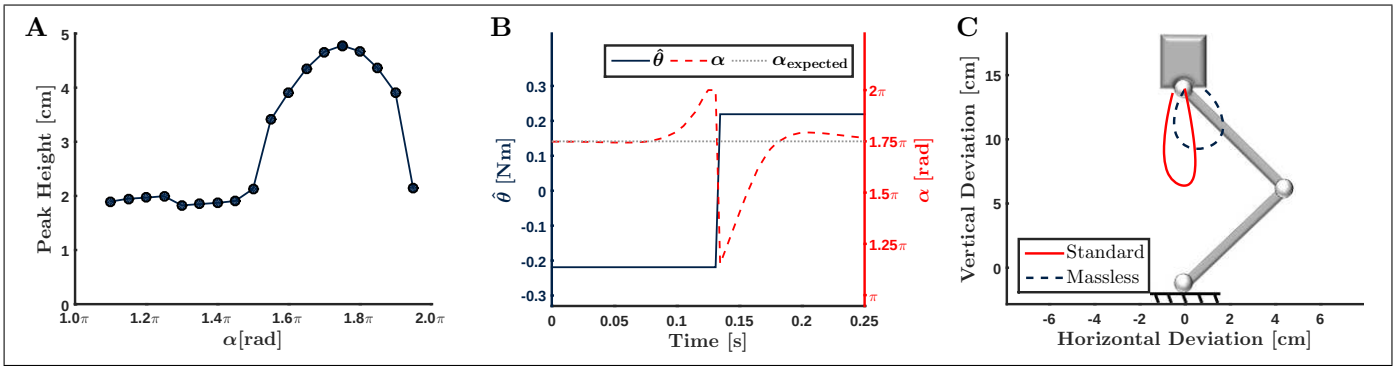

Fig. 2. **(A)** When the optimal control is subject to a pre-defined fixed α, the maximum jumping height varies strongly with the weight angle. The minimum jumping heights are consistently found for $\alpha < 1.5\pi$. This range qualitatively differs from $\alpha > 1.5\pi$, since in the former range both joints share the same sign and one of them will thus always counteract the jumping movement. **(B)** We test the influence of time independency of the transformation weights by allowing for time-dependent weights and search for the controller that maximize the jumping height. The derived control is plotted for one jumping period. Since the control is fixed during the flying phase, only the standing phase is illustrated. The x-axis shows the time that has passed since the onset of the standing phase, not the total simulated time. In agreement with Fig. 1, the controller magnitude $\hat{\theta}$ follows a bang-bang law. The angle $\alpha(t)$ varies continuously with one discontinuous jump from 2π to π, which occurs simultaneously with the sign switch of $\hat{\theta}$. The included reference line shows that the optimal angle agrees with the numerically derived value of $\alpha = 1.75\pi$ at the beginning and the end of the standing phase. **(C)** The trajectory of the base under time-varying weights follows a loop. The dashed line illustrates that it qualitatively remains a loop for massless links, despite quantitative changes.

only $(1,-1)^T$ relates to vertical movement. This agrees with analytic findings by Lakatos et al. [23] who derived the system dynamics with these globally constant eigenvectors of the leg with two mass-less limbs. Based on their derivations, one can transform the damping matrix into the eigenspace and finds that the damping associated to the eigemode $(1,1)^T$ falls below that associated to $(1,-1)^T$ for high deflections. The energy injected into the mode $(1,1)^T$ is transferred into the eigenmode $(1,-1)^T$ via coupling. A significant part of this coupling results from the Coriolis/centrifugal and gravitational force, since the effect qualitatively remains when the masses of the limbs are removed, i.e. the inertia matrix is decoupled in modal coordinates.

V. OPTIMALITY OF OJA'S RULE

Under realistic conditions, the linearized eigenmode of a system is analytically unknown and changes with intrinsic and environmental conditions. In order to maximize the jumping height with minimum energy requirements, our algorithm uses Oja's rule in combination with the modal bang-bang controller to extract an adaptable approximation of the eigenmode from sensory information. In the following, we will evaluate its performance in a simulation and an experiment using parameter screening in combination with a Monte Carlo approach.

A. Methods

Simulation: Our mechanical test bed remains the leg described in Sect. III-A. While the differential equation solver used by GPOPS-II restricted us to a rigid ground model, we here use a more realistic ground model with a stiffness of $10^6\mathrm{N\,m^{-1}}$, a damping coefficient of $2\times10^3\mathrm{N\,s\,m^{-1}}$, and a friction coefficient of 1. We set the bang-bang threshold in (3) to $\epsilon_\tau = 0.5\mathrm{N\,m}$, which we found to prevent decay of the movement for a large parameter range. The time constant of Oja's rule is chosen as $\gamma = 0.1\mathrm{s}^{-1}$. To start the movement, we drop the leg with a vertical distance of $0.02\mathrm{m}$ between foot and ground while the joints are at their equilibrium positions. For the Monte Carlo approach, we assign 40 random 2-tuples to the two remaining free parameters of the model, namely the energy $c_{\epsilon\hat{\theta}}$ injected by the controller and the initial angle α_0 of the transformation weights. The energy $c_{\epsilon\hat{\theta}}$ is drawn from the interval $[0.057\mathrm{N\,m}, 0.563\mathrm{N\,m}]$, which we found to induce stable jumping. For each randomly chosen value $c_{\epsilon\hat{\theta}}$ we empirically derive an interval of values for α that prevent movement decay. An initial angle α_0 is randomly drawn from this interval. During the movement, the weights adjust according to (5). After convergence of the trajectory and weights, the final weight is recorded. We hereby define that the trajectory is converged when the states $(x_{\mathrm{b}2}, q_1, q_2, \dot{q}_1, \dot{q}_2)^T$ at two consecutive peak positions differ by less than $10^{-3}\times(10\mathrm{cm},\ \pi\ \mathrm{rad},\ \pi\ \mathrm{rad},\ \pi\ \mathrm{rad\,s^{-1}},\ \pi\ \mathrm{rad\,s^{-1}})^T$. To verify that our algorithm obtains the dominant principal component of the motion, we perform a reference principal component analysis (PCA) of the joint trajectories using the according *Matlab* function for example trials.

The performance of Oja's rule is validated by parameter screening using 40 additional trials with constant weights described by regularly spaced $\alpha \in [1.5\pi, 2\pi]$ for each value of $c_{\epsilon\hat{\theta}}$. After convergence of the trajectory, we record the respective jumping height. In order to find the peak angle, associated with the peak jumping height, with high accuracy for each value of $c_{\epsilon\hat{\theta}}$, we run 20 additional trials for the subinterval between the three values of α associated with the maximum height. This procedure is repeated for a regularly spaced set of $c_{\epsilon\hat{\theta}} \in [0.057\mathrm{N\,m}, 0.563\mathrm{N\,m}]$.

Experiment: The robotic leg used as experimental setup corresponds to the simulation model, is illustrated in Fig. 4A, and has been previously described by [21]. Two servo units are serially coupled via torsional springs with constant stiffness $k \approx 2\mathrm{N\,m\,rad^{-1}}$ to a hip and a knee joint, respectively. Stiffness was determined using force-deflection measurements. The connection of the second SEA to the knee joint is established via belt drives, resulting in kinematic coupling of the joints. The trunk is mounted to a boom which prevents rotation of

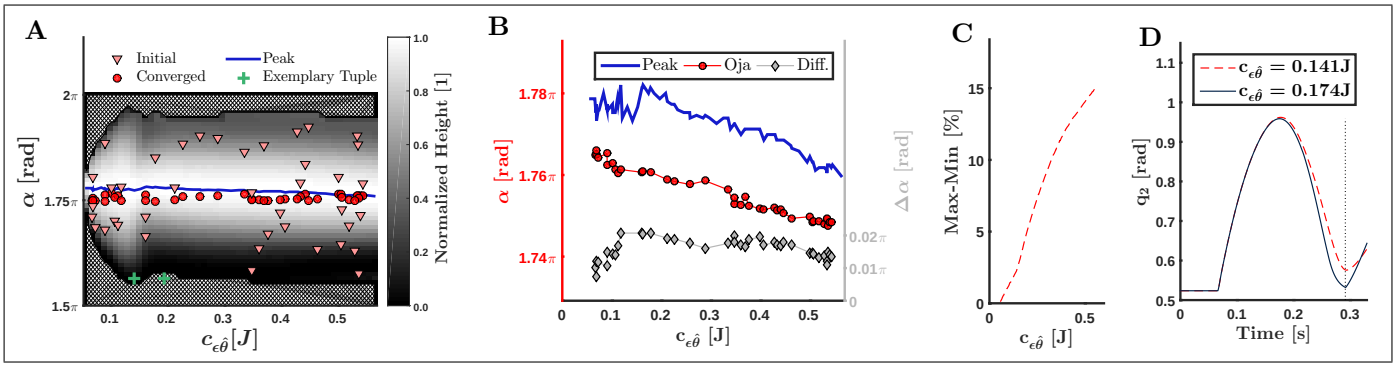

Fig. 3. Simulation results demonstrating the performance of Oja's rule in approximating the local linear eigenmode. **(A)** A parameter screening shows the jumping height as a function of the two free parameters of the bang-bang controller, i.e. the energy $c_{\epsilon\hat{\theta}}$ injected into the system in each jump and the angle α representing the transformation weight vector. The jumping height is normalized for each value $c_{\epsilon\hat{\theta}}$ and the background represents parameter ranges where jumping falls silent. We randomly choose initial tuples $(c_{\epsilon\hat{\theta}}, \alpha_0)$ and initiate jumping of the leg, while the transformation weights adjust according to Oja's rule. The weights converge to values close to the peak line. For values $c_{\epsilon\hat{\theta}} \gtrsim 0.12$J, the range of α that causes stable jumping decreases abruptly, coincident with the transition from oscillations fixed to the ground to a jumping movement. The reason for the abrupt decrease is explained in the text by the two marked exemplary tuples. **(B)** A zoom into the parameter space shows where the converged weights, as obtained by Oja's rule, deviate most from the peak line. We find a minimum deviation for small and large energy input, corresponding to small oscillations without lift-off and large jumping heights. **(C)** For each energy $c_{\epsilon\hat{\theta}}$ within our chosen interval, we show the maximum improvement in jumping height that can be gained by adjusting the transformation weights. Values are given relative to the minimum jumping height when conditions are excluded that cause decay of the movement. **(D)** The trajectory of the knee joint at the beginning of the movement shows qualitative differences for the exemplary tuples marked in sub-figure (A). For larger energy input $c_{\epsilon\hat{\theta}}$, the joint coordinate is not differentiable with respect to time at the marked moment when the leg touches down, indicating removal of kinetic energy. For smaller energy input, the leg remains attached to the ground and thus the joint coordinate remains differentiable.

the trunk while allowing circular horizontal movement around a fixed center and vertical jumping motion. A sensor at the ground fixation point of the boom measures jumping height and horizontal position.

With the motors switched off, we measure the height profile of the ground to correct the jumping height for variations at different horizontal positions. In the beginning, we run the leg using a bang-bang controller with constant weights and wait for the jumping height to converge exponentially while the servo units reach their operating temperature. To prevent overheating, runs lasting 45s are followed by a cooling phase of 120s. At the beginning of each recording sequence, we measure the trunk height while the servos are at rest, $\boldsymbol{\theta} = \mathbf{0}$, and define jumping height relative to this value. An additional height measurement at the end of a recording sequence checks for occurring static hysteresis. We initiate each movement by applying a standardized delta-stimulus and maintain jumping using a bang-bang controller with $\hat{\theta}_z = 0.2\text{rad}$.

In a first recording sequence, we record the trajectory for 10 values of $\alpha \in [1.53\pi, 1.98\pi]$. Each run is followed by a reference run with $\alpha = 1\,75\pi$ to check for repeatability. After convergence of the trajectory, which reliably takes place during the first 10 jumps (cf. example trajectory in Fig. 4B), we average the jumping height for each α.

In a second recording sequence, we initiate α_0 with the minimum and maximum value, $\alpha_{0,\min}$ and $\alpha_{0,\max}$, that allow persistent movement and adapt α according to Oja's rule over several subsequent runs of 45s each. To detect convergence, we average α over each run individually. Convergence is declared when this averaged value is smaller than in the preceding run for trials started with $\alpha_0 = \alpha_{0,\min}$ or larger for trials started with $\alpha_0 = \alpha_{0,\max}$. We measure the respective jumping height that is associated with the initial and final transformation weights twice in an alternating fashion.

B. Results

Simulation: An illustrating overview of the results obtained by the parameter screening and the Monte Carlo approach can be found in Fig. 3A. In Fig. 3B, we zoom into the parameter space to evaluate where the converged weight deviates from the conditions associated with maximum jumping height. We find that the peak angle averaged over the full range of $c_{\epsilon\hat{\theta}}$ amounts to $(1.772 \pm 0.006)\pi$ $(\text{mean} \pm \text{std})$, which significantly deviates from the expectation of $1.750\,\pi$. The peak angle varies slightly as a function of $c_{\epsilon\hat{\theta}}$.

Oja's rule reliably extracts the dominant principal component, as verified in comparison to the PCA performed by Matlab. It closely aligns the randomly chosen initial weights with the peak angle (cf. Fig. 3A). In 36 out of 40 trials, our algorithm improves the transformation weights and leads to an angle that is associated with an increased jumping height. If improvement was purely based on chance, we would expect to find 20 successful trials, distributed according to a binomial distribution. This assumption can be rejected by $p < 10^{-6}$. Thus, Oja's rule significantly improves the energy efficiency of the movement. The closest match between the peak angle and the converged weights are found for small and large input energy levels (cf. Fig. 3B). These energy domains are least affected by the nonlinear switching phase of the hybrid model and can hence be best described by linear dynamics, i.e. the assumption that underlies our controller design. For small energy levels, the system shows only minor deviations from its equilibrium position and stays attached to the ground, indicating that the dynamics can be well approximated by a continuous, linear differential equation. At high energy levels, the dynamics are mostly determined by the flight phase, where the effect of the nonlinear coupling is reduced.

To quantify the improvement that adjustments of the transformation weight yield, we derive the relative difference between

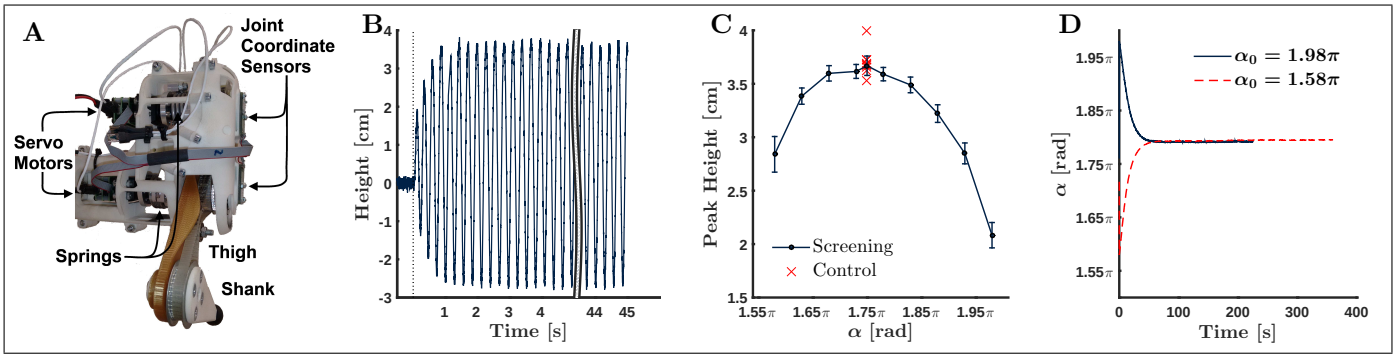

Fig. 4. Results of the experiment. **(A)** The experiments were conducted on a compliant leg that is pictured here. **(B)** An example trunk trajectory. The dotted line indicates the onset of the controller. Fluctuations before this time point illustrate the accuracy of the height sensor. We consistently found that the trajectory converges for less than 10 jumps. **(C)** The average jumping height is plotted as a function of the transformation weights with its peak occurring between $\alpha \in [1.68\pi, 1.78\pi]$. Values of α below the illustrated region lead to a decay of the movement. The parameter space represented in this graph is equivalent to a vertical cross section through Fig. 3A. Each trial is followed by a control recording with $\alpha = 1.75\pi$. The multiple close data points for this value demonstrate that the results are well repeatable throughout the sequence. We averaged them to obtain an additional data point in the screening-curve. Error bars denote the standard deviation over several jumps. **(D)** The transformation weight aligns with the same value under the influence of Oja's rule, independently of the starting conditions. The converged weight lies at the peak of the curve in figure C.

the peak jumping height and the minimum jumping height at each energy value $c_{\epsilon\hat{\theta}}$. Conditions where the leg falls silent are excluded. Figure 3C demonstrates that this difference increases monotonically with $c_{\epsilon\hat{\theta}}$. Within our parameter range, tuning of the transformation weights can lead to relative improvements of more than 15% or $2.6\mathrm{cm}$.

As a final point that may be noticed in Fig. 3A, the range of transformation weights that lead to periodic movement decreases abruptly for values of $c_{\epsilon\hat{\theta}}$ exceeding approximately $0.12\mathrm{J}$. This matches the energy required for lift-off, whereas for smaller energies the leg oscillates with the foot attached to the ground. As shown in in Fig. 3D, the touchdown removes kinetic energy from the system, thereby restricting the range of parameters that prevent decay of the movement.

Experiment: In the physical leg, we find that a small range of weights is related to maximum energy efficiency which cannot sensibly be further divided due to natural fluctuations. Our algorithm extracts weights that lie at this plateau and are independent of the initial conditions, as long as these conditions do not directly lead to movement decay. These results are also illustrated in a supplementary video.

In particular, persistent jumping occurs for $\alpha \in [1.58\pi, 1.98\pi]$. In agreement with the simulation results in Fig. 2A, Fig. 4C demonstrates that the jumping height as averaged over several jumps shows a peak for $\alpha \in [1.68\pi, 1.78\pi]$. In the experimental setup, jumping heights associated with this interval differ by less than one standard deviation from the peak height. Thus, a more accurate peak identification is here prevented due to non-periodicity in the limit cycle, sensor noise, and mistakes in the determination of the height profile of the ground. No static hysteresis is found throughout the recordings and the jumping height of the reference measurements at $\alpha = 1.75\pi$ show no obvious tendency over time and as illustrated in Fig. 4C are consistent throughout the recording sequence. Starting from the weights $\alpha_{0,\mathrm{min}} = 1.58\pi$ and $\alpha_{0,\mathrm{max}} = 1.98\pi$, Oja's rule adjusts the weights to $\alpha_{\mathrm{final,min}} = (1.7950 \pm 0.0002)\pi$ and $\alpha_{\mathrm{final,max}} = (1.7920 \pm 0.0002)\pi$, respectively (cf. Fig. 4D). These values lie exactly at the border of the peak area of Fig. 4C, and the associated jumping heights still differ by less than one standard deviation from the peak height. Whereas the simulation results identify a small but significant deviation between converged and optimal weights, the higher noise therefore renders the differences irrelevant in the experiment. Our trials with initial and converged weights quantify the relative improvement of the jumping height to 31% and 67%, respectively. The latter corresponds to an absolute improvement of $1.4\mathrm{cm}$.

VI. DISCUSSION

We recently suggested a computationally simple control approach that induces stable periodic movement in elastic multibody systems. The present paper concentrates on the proposed system-specific time-independent linear transformation between the joint space and a one-dimensional controller space. While a modal transformation is analytically known to be optimal in terms of energy efficiency for mechanical systems with continuous linear dynamics, we here investigate its performance in the control of resonance in hybrid dynamical systems with nonlinear coupling between the joints. We show that a previously proposed algorithm can use sensory information about joint deflections to extract transformation weights that induce limit cycles of energy efficiency which is indistinguishable from an optimal trajectory for noisy physical systems. This finding is independent of the initial weights.

The simulation results show two shortcomings of our algorithm: Firstly, optimal transformation weights vary during the movement cycle, which improves the performance in the single-digit percentage area. This small increase can be expected to be irrelevant for applications in experimental systems, where model-based optimal control laws suffer from deficits in the underlying model. Furthermore, the difference has minor influence on the jumping height in comparison to adaptations by our (model-free) adaptation law, since the latter can increase the height by several magnitudes. Secondly, our Monte Carlo approach demonstrates that Oja's rule does not precisely extract the optimal linear weights. However, our extracted weights lie on a peak plateau of weights whose mutual

difference in jumping height is obscured by fluctuations due to intrinsic noise of the system.

In accordance with earlier research, the present study focuses on bang-bang controllers. This choice is due to their previously demonstrated robustness properties and the ability to generate asymptotically stable limit cycles. Our algorithm leads to higher relative improvements for a smaller bang-bang threshold, as this decreases the minimum energy required for persistent movement, which lowers the minimum, i.e. reference, jumping height. Thus, we find a smaller relative, but similar absolute, increase in the jumping height in the simulations in comparison to the experiments with smaller threshold. Our experiments show high performance increases of up to 68% and potentially more for higher energy input.

We concentrate on a jumping leg since highly dynamical locomotion is a promising beneficiary of compliant structures due to the high power demands and occurring peak forces. Two findings render our algorithm especially advantageous for this motion type: On the one hand, the optimization of constant weights yields higher improvements here, presumably because higher forces allow elastic elements to store more energy. On the other hand, Oja's rule extracts optimal weights with increasing accuracy at higher motion amplitude.

Oja's rule is widely known as description for calculations performed by the animal nervous system [10], [13]. Furthermore, the presented control approach leads to highly stable motion. Based on these aspects, we previously suggested that the approach may describe aspects of the sophisticated movement control of animals [10], [16]. The obtained strong and reliable increase in jumping performance the we find here emphasizes our hypothesis that it describes neural calculations as shaped by evolutionary constraints.

Our present focus lies on the energy used for mechanical actuation. Our algorithm is additionally energy-efficient in terms of computational power requirements and sensing hardware. While other previously suggested adaptable controllers spend a significant amount of energy for these purposes [24], the calculations of our algorithm are computationally simple and require to store only the modal transformation weights during execution, while information about joint forces and deflections suffice as sensory input.

Future work on the control of elastic multibody systems may use the modular nature of our coordinate transformation, which adjusts a low-dimensional control signal to yield an energy-efficient movement of several joints without constraints on the signal. In the controller sub-manifold, a modular controller may combine commands for non-energetic purposes that have different origins, such as sensory and internally generated signals. Such a controller may also produce two-dimensional commands that target different limbs in anti-phasic gaits like running without considerations about individual joints.

ACKNOWLEDGMENT

Thanks to D. Seidel for infrastructural work on the robot.

REFERENCES

[1] T. Buschmann, A. Ewald, A. von Twickel, and A. Buschges, "Controlling legs for locomotion - insights from robotics and neurobiology," *Bioinspir Biomim*, vol. 10, no. 4, p. 041001, Aug 2015.

[2] K. Sreenath, H.-W. Park, I. Poulakakis, and J. Grizzle, "A compliant hybrid zero dynamics controller for stable, efficient and fast bipedal walking on MABEL," *Int J Robot Res*, 2010.

[3] A. Shiriaev, L. Freidovich, and I. Manchester, "Can we make a robot ballerina perform a pirouette? Orbital stabilization of periodic motions of underactuated mechanical systems," *Annu Rev Control*, vol. 32, pp. 200–211, Jul 2008.

[4] D. J. Braun, M. Howard, and S. Vijayakumar, "Exploiting variable stiffness in explosive movement tasks," in *Robotics: Science and Systems VII*, Los Angeles, CA, USA, June 2011.

[5] G. Garofalo, C. Ott, and A. Albu-Schäffer, "Orbital stabilization of mechanical systems through semidefinite Lyapunov functions," in *2013 American Control Conference*, June 2013, pp. 5715–5721.

[6] S. Stramigioli and M. van Dijk, "Energy conservation limit cycle oscillations," in *International Federation Of Automatic Control, Proceedings Of The 17th World Congress*, 2008, pp. 15 666–15 671.

[7] T. Nachstedt, F. Wörgötter, and P. Manoonpong, "Adaptive neural oscillator with synaptic plasticity enabling fast resonance tuning," in *Artificial Neural Networks and Machine Learning at ICANN 2012*, A. Villa, W. Duch, P. rdi, F. Masulli, and G. Palm, Eds. Springer Berlin Heidelberg, 2012, vol. 7552, pp. 451–458.

[8] X. Xiong, F. Wörgötter, and P. Manoonpong, "Adaptive and energy efficient walking in a hexapod robot under neuromechanical control and sensorimotor learning," *Cybernetics, IEEE Transactions on*, vol. PP, no. 99, 2015.

[9] J. Buchli and A. J. Ijspeert, "Self-organized adaptive legged locomotion in a compliant quadruped robot," *Autonomous Robots*, vol. 25, no. 4, pp. 331–347, 2008.

[10] P. Stratmann, D. Lakatos, and A. Albu-Schäffer, "Neuromodulation and synaptic plasticity for the control of fast periodic movement: Energy efficiency in coupled compliant joints via PCA," *Front Neurorobot*, vol. 10, no. 2, 2016.

[11] D. Lakatos, M. Gorner, F. Petit, A. Dietrich, and A. Albu-Schäffer, "A modally adaptive control for multi-contact cyclic motions in compliantly actuated robotic systems," in *Intelligent Robots and Systems, 2013 IEEE/RSJ Intl Conf on*, 2013, pp. 5388–5395.

[12] D. Lakatos, F. Petit, and A. Albu-Schäffer, "Nonlinear oscillations for cyclic movements in human and robotic arms," *Robotics, IEEE Transactions on*, vol. 30, no. 4, pp. 865–879, Aug 2014.

[13] E. Oja, "Simplified neuron model as a principal component analyzer," *Journal of Mathematical Biology*, vol. 15, no. 3, pp. 267–273, 1982.

[14] K. D. Miller and D. J. C. MacKay, "The role of constraints in Hebbian learning," *Neural Computation*, vol. 6, pp. 100–126, 1994.

[15] D. Lakatos and A. Albu-Schäffer, "Switching based limit cycle control for compliantly actuated second-order systems," in *Proceedings of the IFAC World Congress*, vol. 19, no. 1, 2014, pp. 6392–6399.

[16] D. Lakatos and A. Albu-Schäffer, "Neuron model interpretation of a cyclic motion control concept," in *5th IEEE Intl Conf on Biomedical Robotics and Biomechatronics*, Aug 2014, pp. 905–910.

[17] B. Feeny and R. Kappagantu, "On the physical interpretation of proper orthogonal modes in vibrations," *J. Sound Vibration*, vol. 211, no. 4, pp. 607 – 616, 1998.

[18] G. Kerschen and J. C. Golinval, "Physical interpretation of the proper orthogonal modes using the singular value decomposition," *Journal of Sound and Vibration*, vol. 249, no. 5, pp. 849 – 865, 2002.

[19] G. Kerschen, J.-c. Golinval, A. F. Vakakis, and L. A. Bergman, "The method of proper orthogonal decomposition for dynamical characterization and order reduction of mechanical systems: An overview," *Nonlinear Dynamics*, vol. 41, no. 1, pp. 147–169, 2005.

[20] M. A. Patterson and A. V. Rao, "GPOPS-II: A MATLAB software for solving multiple-phase optimal control problems using hp-adaptive Gaussian quadrature collocation methods and sparse nonlinear programming," *ACM Trans. Math. Softw.*, vol. 41, no. 1, pp. 1:1–1:37, oct 2014.

[21] D. Lakatos, D. Seidel, W. Friedl, and A. Albu-Schäffer, "Targeted jumping of compliantly actuated hoppers based on discrete planning and switching control," in *Intelligent Robots and Systems (IROS), 2015 IEEE/RSJ Intl Conf on*, Sept 2015, pp. 5802–5808.

[22] T. L. Wächter, Andreasand Biegler, "On the implementation of an interior-point filter line-search algorithm for large-scale nonlinear programming," *Math Program*, vol. 106, no. 1, pp. 25–57, 2005.

[23] D. Lakatos, W. Friedl, and A. Albu-Schäffer, "Modal dynamics matching: embodying fundamental locomotion modes into legged robots with elastic elements," Submitted to RA-L/ICRA, 2017.

[24] Y. Mei, Y.-H. Lu, Y. C. Hu, and C. S. G. Lee, "A case study of mobile robot's energy consumption and conservation techniques," in *ICAR, 12th Intl Conf on Advanced Robotics*, July 2005, pp. 492–497.